



# Quantifying rhizosphere priming effects on soil organic matter decomposition *in situ* in a subarctic ecotone using natural abundance radiocarbon

5 <sup>1</sup>Louis Mielke\*, <sup>1,2</sup> Thomas Parker\*, <sup>3</sup>Lorna Street, <sup>4</sup>Karina Clemmensen, <sup>1,5</sup>Nina Lindstrom Friggens, <sup>6</sup>Mark Garnett, <sup>5</sup>Iain Hartley, <sup>7</sup>David Johnson, <sup>1</sup>Jens-Arne Subke, <sup>1</sup>Philip Wookey.  
\*Contributed equally

<sup>1</sup>School of Life and Environmental Sciences, University of Stirling, Stirling, FK9 4LA, Scotland, UK

10 <sup>2</sup>Ecological Sciences, The James Hutton Institute, Aberdeen, AB15 8QH, Scotland, UK

<sup>3</sup>School of GeoSciences, University of Edinburgh, Edinburgh, EH9 3FF, Scotland, UK

<sup>4</sup>Department of Forest Mycology and Plant Pathology, Swedish University of Agricultural Sciences, Uppsala SE-75007, Sweden

<sup>5</sup>Geography, Faculty of Environment, Science and Economy, University of Exeter, Exeter, EX4 4RJ, UK

15 <sup>6</sup>NEIF Radiocarbon Laboratory, SUERC, East Kilbride, G75 0QF, Scotland, UK

<sup>7</sup>Lancaster Environment Centre, Lancaster University, Bailrigg, LA1 4YQ, UK

Correspondence to: Louis Mielke ([louis.mielke@stir.ac.uk](mailto:louis.mielke@stir.ac.uk)), Thomas Parker ([thomas.parker@hutton.ac.uk](mailto:thomas.parker@hutton.ac.uk))

20 **Abstract.** Changes in plant-soil interactions associated with shifts in vegetation composition and climate change may have a range of effects on soil microbial activity, including increases (positive priming), inhibition (negative priming), or no net change in organic matter decomposition. The carbon-rich soils, including peats, of high latitude ecosystems, in particular, are at risk of large carbon losses linked to ongoing vegetation shifts, yet their vulnerability to priming *in situ* remains unresolved. Here we deploy a field-based technique, which harnesses the contemporary atmosphere as a radiocarbon (<sup>14</sup>C) ‘label’ together  
25 with a <sup>14</sup>C-depleted (‘ancient’) peat substrate, to quantify soil organic matter (SOM) decomposition in the presence or absence of roots and rhizosphere processes in subarctic Sweden. Collars encased with different mesh sizes were placed in control and girdled (in which belowground carbon transport from the plant canopy was disrupted) mountain birch forest and willow shrub stands to test the hypothesis that the presence of ectomycorrhizal roots and extra-radical mycorrhizal mycelium increases SOM decomposition through positive priming. As expected, carbon dioxide (CO<sub>2</sub>) and dissolved organic carbon (DOC) from root  
30 ingrowth cores were significantly enriched in <sup>14</sup>C (contemporary carbon) compared to CO<sub>2</sub> and DOC from root exclusion cores (peat carbon), allowing partitioning of carbon mobilisation between heterotrophic (peat substrate) and recent autotrophic (plant) sources. Neither vegetation community (birch or willow), nor girdling treatment, were statistically significant as main effects, but there was a significant rhizosphere priming effect ratio of 1.36 across all groups; thus, the ancient peat-derived CO<sub>2</sub> flux was 36% higher in the presence of a rhizosphere than when it was absent. The lack of a significant girdling effect  
35 did not support our specific hypothesis that the presence of ectomycorrhizal roots and their associated mycelium increases SOM decomposition, but the substantial variability of modelled ancient CO<sub>2</sub> efflux and DOC concentration during the peak



growing season is consistent with the existence of ‘hot-spots’ of microbial activity. Our study provides a potential alternative to artificial substrate (e.g. glucose) additions, or  $^{13}\text{C}$  labelling (e.g. pulse-chase), to estimate priming in ecosystems. Furthermore, the study, undertaken *in situ* in the subarctic, emphasizes that increased primary productivity and associated rhizosphere processes, associated with shifts in vegetation composition and climate change, may not translate simply into increased C sequestration at whole-ecosystem scale.

## 1 Introduction

The net carbon (C) balance of Northern Hemisphere terrestrial high latitudes has a large potential influence on global climate. Warmer temperatures, longer growing seasons and atmospheric  $\text{CO}_2$  enrichment all act to increase plant growth, thus increasing uptake of  $\text{CO}_2$  by the vegetation. However, increased plant growth and shifting vegetation composition can also influence soil organic matter (SOM) decomposition via rhizosphere processes such as priming. Broadly, rhizosphere priming commonly refers to an increase in pre-existing SOM decomposition (positive priming) in the presence of roots, root-associated microorganisms, and labile carbon inputs from roots (Huo et al., 2017). It should be noted, however, that in soils with limited C availability, for example when dominated by low and/or recalcitrant SOM stocks, negative priming has also been observed (Siles et al., 2022; Mueller and Megonigal, 2024), whereby microorganisms shift from decomposing pre-existing SOC to mineralizing the added fresh carbon due to preferential substrate utilization. Thus, priming can range from positive to negative, or none, and the related mechanistic links between vegetation change at high latitudes, and rates of decomposition of SOM, remain poorly understood. This uncertainty limits our ability to predict the future C balance of terrestrial ecosystems both here and globally.

The northern high latitudes are warming more rapidly than the global average; indeed, the Arctic region is estimated to have warmed nearly four times faster than the globe since 1979 (Rantanen et al., 2022). Furthermore, tundra and taiga ecosystems store ~351 and 811 Pg C in the top 30, and 100 cm, respectively, representing around 1/3<sup>rd</sup> of the global soil C stock (Kuhry et al., 2013). Increases in temperature, thaw depth and lengthening growing seasons all potentially create more favourable soil conditions, both for SOM decomposition and plant root activity. Aboveground, evidence of change in vegetation composition and productivity is clear, with large-scale increases in tall shrub cover and advances of the forest line, both northwards and to higher altitudes (Dial et al., 2024; Rees et al., 2020). Increasing plant growth and the shift towards woody species may amplify potential rhizosphere priming effects as plants allocate more C belowground. Indeed, in some parts of the Arctic, areas of higher shrub and tree abundance are associated with lower soil C stocks compared to neighbouring tundra (Parker et al., 2015; Wilmking et al., 2006), possibly reflecting faster soil C turnover linked to positive rhizosphere priming (Hartley et al., 2012). However, the magnitude of rhizosphere priming effects on SOM decomposition have never been directly quantified *in situ* in high latitude ecosystems. This represents a critical knowledge gap – high latitude soil carbon stocks are so large that even



relatively small increases in C losses may tip the circumpolar north from being a net sink to a source, despite increasing net primary productivity (Braghiere et al., 2023).

70

Most trees and shrubs found in the Arctic rely on ectomycorrhizal symbionts for nutrient acquisition, to which they allocate carbon to fuel mycelial exploration of the soil (Smith and Read, 2008). Within ectomycorrhizal fungi there is a considerable potential to produce extracellular enzymes that can degrade SOM, depending on the species (Read and Perez-Moreno, 2003; Lindahl and Tunlid, 2015; Miyauchi et al., 2020). Therefore, enhanced decomposition in the presence of mycorrhizal roots and fungi could be considered a soil priming mechanism, especially in the context of nitrogen mining whereby ectomycorrhizal species may degrade SOM and selectively extract N (Clemmensen et al., 2021). It should be noted, however, that saprotrophic fungi also play a central role in the breakdown of SOM, and competition between these two fungal guilds has been hypothesized to lead to suppression of decomposition rates in a phenomenon known as the ‘Gadgil effect’ (Fernandez and Kennedy, 2016), which could be considered an instance of negative priming. Furthermore, soil fauna are stimulated by root and rhizosphere processes, which can lead to an increased density and biomass of organisms associated with decomposition (Bardgett and Cook, 1998; Zuev et al., 2023). Our understanding of rhizosphere priming effects therefore needs to be built on *in situ* quantification which includes the full complexity of soil communities associated with plant hosts.

80

Several approaches have been applied to quantify SOM priming (Kuzyakov, 2010; Bernard et al., 2022), with most priming experiments conducted in the laboratory (e.g. Wild et al. (2016)), owing to the technical difficulty of measuring priming *in situ*. There have also been a range of field-based approaches to investigate interactions of organic matter decomposition under modified rhizosphere carbon supply, often utilising stable isotope tracers ( $^{13}\text{C}$  or  $^{15}\text{N}$ ) to understand *in situ* carbon turnover (Paterson et al., 2009). Priming studies using intact natural vegetation are rare, owing to the technical difficulties of implementing experimental manipulations of complex ecosystems that allow the identification of carbon turnover processes and  $\text{CO}_2$  flux contribution from different sources within the plant-soil system. Using natural abundance of  $^{14}\text{C}$  in organic matter to partition sources of  $\text{CO}_2$  has recently been demonstrated for intact Arctic shrub communities (Street et al., 2020), providing a promising approach for cold-climate ecosystems typically dominated by long-lived woody perennials or mature canopy-forming trees with extensive mycorrhizal colonisation.

90

In this study we quantified root and rhizosphere priming effects *in situ* at a mountain birch forest in an arctic-alpine treeline ecotone in northern Sweden. We deployed a novel field-based method which exploits the distinct  $^{14}\text{C}$  signature of a ~2700-year-old peat to partition respiration sources in the presence and absence of roots and mycorrhizal fungi. To investigate the impact of tall shrubs and trees on priming, we compared priming effects between intact vegetation and experimentally girdled plots in which belowground carbon transport from the plant canopy had been disrupted (Parker et al., 2020). This work showed that girdling reduced soil respiration, root production and mycelium production, together resulting in a reduction in root and rhizosphere activity, reflecting reduced C allocation to roots and rhizosphere processes (Parker et al., 2020). Therefore, we

100

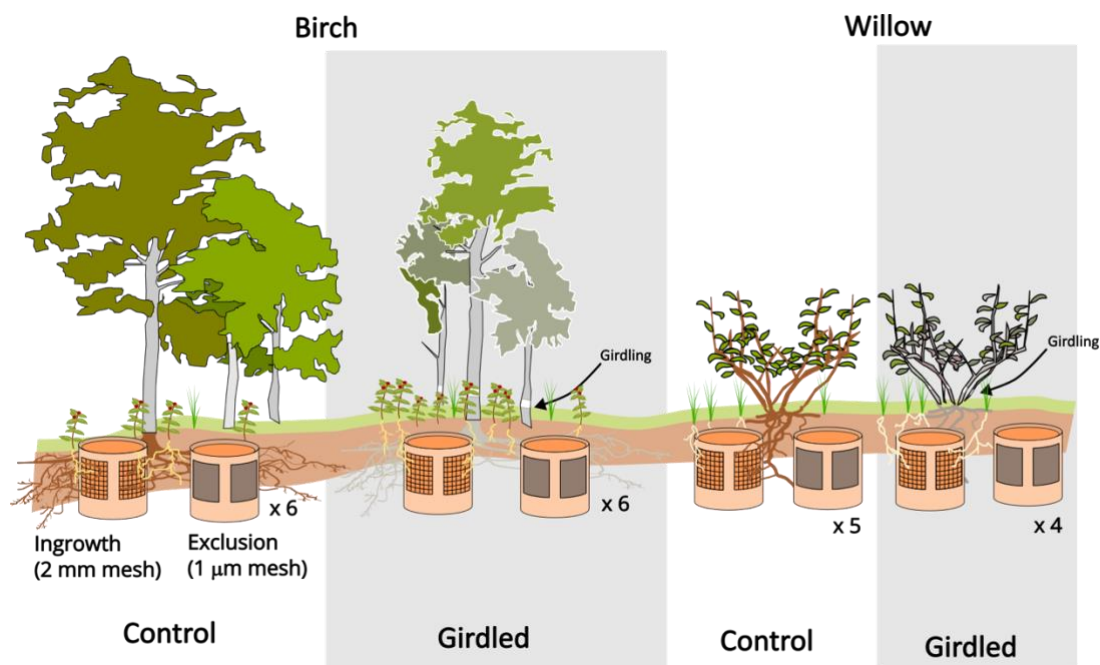


hypothesize 1) that presence of roots and associated organisms increases SOM decomposition (positive priming), and 2) that this priming effect is greater in ungirdled plots (with intact ectomycorrhizal shrubs and canopy trees) than in girdled plots, with only understorey vegetation.

## 105 2 Materials and Methods

### 2.1 Site and Experimental Design

We utilised a girdling experiment around a permafrost-free forest tundra ecotone 4 to 5 km south of the Abisko Scientific Research Station, Sweden (68°18'N 18°49'E), at ~ 600 m a.s.l. (Figure 1; see Parker et al. (2020) for details). Briefly, six pairs of plots in mountain birch (*Betula pubescens* Ehrh. ssp. *czerepanovii* (Orlova) Hämet Ahti) forest, and five pairs of plots in woolly willow (*Salix lapponum* L.) thickets, were located across a 0.88-km<sup>2</sup> area within the treeline ecotone. At Abisko Research Station (356 m a.s.l.), the mean January and July temperatures were -10.9 and +10.3°C, respectively, and the mean annual precipitation was 1014 mm from 1991 to 2020 (Hersbach, 2023). Soils consist of a well-developed organic layer, an albic horizon indicative of leaching, and a silt-rich lower-mineral horizon with a pH between 4.0 and 5.6, over glacial till deposits. The understorey vegetation of the mountain birch forest is dominated by ericaceous species, mainly *Empetrum* 115 *nigrum* L. ssp. *hermaphroditum* (Hagerup) Böcher and *Vaccinium vitis-idaea* L., with occasional patches of *V. myrtillus* L. and abundant bryophytes. Understorey vegetation of the willow plots included graminoids and a smaller portion of *Betula nana* L.. In June 2017, one member of each pair of birch or willow stands was randomly selected to be girdled. In willow plots, all willow stems within a 2-m radius were girdled; the epidermis, periderm, cortex and phloem were removed in a continuous ~4-8 cm wide band around the stem, as close to the base as possible. The plot perimeters of both girdled and control plots were 120 trenched with plastic sheet to prevent root ingrowth from outside the plots. In forest plots, every birch tree within a 10-m radius was girdled. Girdling was found to be highly effective in reducing bulk soil respiration in both birch and willow plots.



125 **Figure 1. Birch and willow plots with girdled and control treatments.** Peat substrate was contained within PVC collars with windows of different mesh sizes to allow (2-mm mesh) or restrict (1- $\mu$ m mesh) root and hyphal growth into the peat within control and girdled treatments. Any priming effects were hypothesized to be greater in Control (ungirdled) plots, with intact ectomycorrhizal shrubs and canopy trees, than in Girdled plots, with only understorey vegetation contributing to below-ground C fluxes through rhizodeposition.

## 2.2 $^{14}\text{C}$ -depleted Mesh Soil Cores

130 In July 2017, peat was excavated from 55 to 100 cm depth from a small island on lake Uddjaure, Sweden (65° 56' 52.8", 17° 50' 45.6"), retained at field moisture and passed through a 4-mm sieve (pH 3.5-3.7). To assess the radiocarbon activity (%modern) of the peat, a representative sub-sample was combusted by heating with CuO in a sealed quartz glass tube and recovered as CO<sub>2</sub> following cryogenic purification (Boutton et al., 1983). The gas was converted to graphite by Fe/Zn reduction prior to analysis by Accelerator Mass Spectrometry (AMS; Ascough et al. 2024). This sample had an average  $^{14}\text{C}$  content of  
135 71.41% modern carbon (Table 1). Washed sand (carbonate-free) from the shores of Lake Torneträsk (68° 23' 45.6", 18° 49' 30") was homogenized with Uddjaure peat 1:1 (v:v) to increase drainage, provide structure and limit shrinking. Between 1<sup>st</sup> and 3<sup>rd</sup> of August 2017, in each experimental plot, two 16 cm diameter soil cores were removed to the depth of 14 cm and replaced by two PVC cylinders of the same diameter (16 cm height) and containing the  $^{14}\text{C}$ -depleted Uddjaure peat (subsequently referred to as a 'peat core'). The cores were inserted so that the peat surface was flush with the surrounding soil,  
140 leaving 2 cm of PVC standing above the soil surface. The time between peat extraction and peat core installation was 14 days. Three windows (12 cm wide, 3 cm high) were cut into the side of each PVC core such that the upper edge of each window was 4 cm below the upper edge of each core, i.e. 2 cm below the soil surface. To separate autotrophic (roots and rhizosphere processes) from free-living heterotrophic components, windows were covered by nylon mesh with mesh sizes of either 2-mm



(ingrowth core) or 1- $\mu$ m (exclusion core) (Fig 1.). Mesh of corresponding size was also fixed to the bottom of the core to  
145 prevent waterlogging while allowing or excluding ingrowth from below. Window size and position was determined to  
maximise root ingrowth (spanning over 70% of the circumference of cores) while maintaining structural integrity of the  
cylinder. A 2-mm white mesh was placed on the soil surface inside each core to intercept falling leaf litter and other debris,  
and material was removed from this mesh regularly to restrict recent C inputs from above. The surface mesh also acted to limit  
exposure of the soil to direct sunlight and limit surface drying. Newly colonising mosses and seedlings were picked from the  
150 surface continuously; no seedling grew to more than 1-2 cm.

### 2.3 Respired $^{14}\text{C}$ sample collection and $^{14}\text{C}$ determination

In the last week of July 2021, after 4 years of deployment, soil cores were removed for  $\text{CO}_2$  and DOC sampling and radiocarbon  
determinations. July is considered peak growing season in this subarctic location, when maximum rhizosphere priming effects  
155 are anticipated. However, the  $\text{CO}_2$  and DOC sampling and radiocarbon collections were originally scheduled for the previous  
(2020) growing season, but the COVID-19 pandemic resulted in deferral until 2021.

The peat cores were cut around with a sharp knife, leaving 2 cm of adhering soil, and lifted out with a spade. Once out of the  
ground, soil external to the core was carefully removed and in-grown roots were trimmed to the outer surface of mesh windows,  
160 leaving only roots that had grown into the peat. Each core was then placed in a sealed 10-l plastic box fitted with PTFE tubing  
to monitor  $\text{CO}_2$  build-up. Paired cores from each plot were incubated simultaneously in boxes placed in the shade and covered  
with reflective bubble-wrap to limit heating during the  $\text{CO}_2$  collections and flux measurements.

After sealing boxes,  $\text{CO}_2$  was initially removed by circulating air through a soda lime column for 30 to 40 minutes at a rate of  
165  $500 \text{ ml min}^{-1}$  to reduce contributions from atmospheric  $\text{CO}_2$ . This scrubbing process reduced  $\text{CO}_2$  concentrations to between  
200 and 300 ppm. Carbon dioxide efflux rates were subsequently measured by monitoring the increase in  $\text{CO}_2$  concentration  
(IRGA, EGM-5, PP Systems) within the closed system over a 5-minute period.  $\text{CO}_2$  was then allowed to build up further to  
between 800 and 2000 ppm to collect at least 3 ml of  $\text{CO}_2$  on a molecular sieve trap (placed inline and pumped at  $500 \text{ ml}$   
 $\text{min}^{-1}$ ), following the methods of Garnett et al. (2021). The  $\text{CO}_2$  build-up phase took between 2 and 4 hours for the rooted peat  
170 cores (ingrowth), but up to 12 hours for the heterotroph-only (exclusion) peat cores, owing to lower respiration rates in the  
latter. Method validation for the longevity of the root and rhizosphere respiration after root severing can be found in Appendix  
A. Molecular sieve traps were returned to the NEIF Radiocarbon Laboratory (East Kilbride, Scotland) where the  $\text{CO}_2$  was  
recovered by heating and cryogenic collection, followed by graphitisation and  $^{14}\text{C}$  measurement by AMS (Ascough et al.,  
2024). Radiocarbon concentrations were normalised to a delta- $^{13}\text{C}$  of -25‰ to account for any mass dependent isotopic  
175 fractionation effects (Gaudinski, 2000; Stuiver and Polach, 1977), and are presented as %modern, calculated as %modern =



$\frac{R_{sample}}{R_{modern}} \times 100$ , where  $R$  is the  $^{14}\text{C}/^{12}\text{C}$  ratio of a sample or modern reference (Oxalic acid II, National Institute of Standards and Technology, USA), respectively.

## 2.4 Radiocarbon activity of respired Uddjaure peat

180 For partitioning respiration sources (see Section 2.7, below), we obtained a sample of  $\text{CO}_2$  respired from the Uddjaure peat during incubation *in vitro* in the laboratory. This was collected in the absence of atmospheric and autotrophic sources of C and represents metabolism of heterotrophic organisms. The peat soil was incubated between  $\sim 11$  and  $16^\circ\text{C}$  from August 2017 to achieve a basal rate of respiration. The incubation vessel was sealed on 6 December 2017 and atmospheric  $\text{CO}_2$  removed by scrubbing with soda lime. Evolved  $\text{CO}_2$  was collected by pumping the headspace gases through a molecular sieve trap after  
185 sufficient  $\text{CO}_2$  ( $>3$  ml) had accumulated for  $^{14}\text{C}$  analysis (9 January 2018) and processed using methods as described in section 2.3.

## 2.5 Correction for atmospheric contamination

We determined  $\delta^{13}\text{C}$  of respired  $\text{CO}_2$  ( $\delta^{13}\text{C}_{sample}$ ) from ‘Keeling plots’ as the y-intercept of the inverse of the sampled  $\text{CO}_2$  concentration plotted against the  $\delta^{13}\text{C}$  value from AMS analysis separately for the ingrowth and exclusion cores (see Appendix  
190 B; Fig B1; (Gaudinski, 2000; Street et al., 2020). To account for atmospheric contamination of the  $\text{CO}_2$  samples, we calculated the fractional contribution of atmospheric  $\text{CO}_2$  ( $f_{air}$ ) to each  $\text{CO}_2$  sample based on a two-source mixing model with the  $\delta^{13}\text{C}_{\text{CO}_2}$  of air ( $\delta^{13}\text{C}_{air}$ ) and the  $\delta^{13}\text{C}_{\text{CO}_2}$  of Uddjaure peat respiration ( $\delta^{13}\text{C}_{peat}$ ) as end members (Eq. 1).

$$f_{air} = \frac{(\delta^{13}\text{C}_{sample} - \delta^{13}\text{C}_{peat})}{(\delta^{13}\text{C}_{air} - \delta^{13}\text{C}_{peat})} \quad (1)$$

195

Atmospheric C isotopic signatures were determined from three air samples collected on molecular sieve from the first two growing seasons (2017 and 2018) after the peat cores were established, and the final season (2021) when the peat cores were harvested. The  $^{14}\text{C}$  content of the respired  $\text{CO}_2$  efflux ( $\Delta_{resp}$ ) was then calculated using Equation 2:

200

$$\Delta_{resp} = \frac{(\Delta_{sample} \times 1) + (\Delta_{air} \times f_{air})}{1 - f_{air}} \quad (2)$$

Where  $\Delta_{sample}$  is the sampled  $^{14}\text{CO}_2$  signature (%modern),  $\Delta_{air}$  represents the atmospheric  $^{14}\text{CO}_2$  signature (%modern) at the time of sampling (2021), and  $\Delta_{resp}$  is the  $^{14}\text{C}$  content of respiration from the ingrowth or exclusion peat cores.



## 205 2.6 DO<sup>14</sup>C sample collection and processing

All peat cores were taken to the laboratory within 24 h of CO<sub>2</sub> collection for dissolved organic C extraction. Ingrown roots in the peat cores with 2-mm mesh were picked out by hand, washed, oven dried at 70°C for 48 h, and weighed. From the homogenised peat-sand matrix, 200 g (fresh weight) was added to 500 ml of deionised Millipore water, mixed by hand for 10 seconds and left to settle for 10 minutes. 400 ml of supernatant was then filtered through a glass fibre filter (Whatman GFF) into a polycarbonate bottle and maintained at 4°C. Prior to analysis, the DOC extracts were freeze-dried, acid-fumigated, combusted to CO<sub>2</sub>, converted to graphite and analysed for <sup>14</sup>C by AMS (Ascough et al. (2024) at the NEIF Radiocarbon Laboratory (East Kilbride, Scotland).

## 2.7 Partitioning respiration sources

215 To quantify the influence of root and rhizosphere processes on the rate of decomposition of the incubated peat, we used the <sup>14</sup>C content to partition the respiration from each peat core into CO<sub>2</sub> derived from (1) recent plant-derived carbon and (2) peat-derived carbon (Subke et al., 2003; Street et al., 2020). The fractional contribution of respiration from peat-derived carbon ( $f_{peat}$ ) was calculated based on a two-source mixing model:

$$220 \quad f_{peat} = \frac{(\Delta_{resp} - \Delta_{recent})}{(\Delta_{peat} - \Delta_{recent})} \quad (3)$$

where  $\Delta_{resp}$  is the <sup>14</sup>CO<sub>2</sub> content of respiration from the entire soil core,  $\Delta_{peat}$  is the <sup>14</sup>CO<sub>2</sub> content of respiration from the peat and  $\Delta_{recent}$  is the <sup>14</sup>C content of the recently photosynthesised carbon (%modern), which we assume is equal to the <sup>14</sup>C signature of the atmosphere in 2021. Finally, the modelled peat-derived CO<sub>2</sub> flux from each soil core ( $F_{peat}$ ;  $\mu\text{mol m}^{-2} \text{s}^{-1}$ ) was calculated as the product of the observed CO<sub>2</sub> flux from the core ( $F_{total}$ ) and the estimated peat-derived fraction ( $f_{peat}$ ):

$$225 \quad F_{peat} = F_{total} \times f_{peat} \quad (4)$$

We then calculated the rhizosphere priming effect (RPE) for each plot as:

$$230 \quad RPE = \frac{F_{peat \text{ ingrowth}}}{F_{peat \text{ exclusion}}} \quad (5)$$

Where  $F_{peat \text{ ingrowth}}$  is the peat derived CO<sub>2</sub> flux in the 2-mm mesh cores and  $F_{peat \text{ exclusion}}$  is the peat derived CO<sub>2</sub> flux in the 1- $\mu\text{m}$  mesh cores from the same plot, excluding roots.

235



## 2.8 Statistical analysis

The effects of girdling and the presence of roots and rhizosphere processes were tested as explanatory factors for the total, recently plant-derived, and ancient peat-derived CO<sub>2</sub> fluxes, <sup>14</sup>CO<sub>2</sub> signatures (%modern), DOC concentrations (mg L<sup>-1</sup>) and DO<sup>14</sup>C signatures (%modern) using mixed effects linear models from the nlme package (version 3.1) in R (version 4.4.1) for each vegetation type separately. The treatment (control or girdled) and mesh size (1-μm = Exclusion, or 2-mm = Ingrowth) were designated fixed effects, and the plot designated a random effect to account for plot level differences arising from spatial variation. We tested the effect of vegetation type and girdling on RPE ratios using fixed effects linear models in R (version 4.4.1). Response variables were natural log (ln(x)) transformed to maintain homoscedasticity.

## 3 Results

### 3.1 Atmospheric <sup>14</sup>CO<sub>2</sub> and <sup>14</sup>C signature of ancient peat

Atmospheric <sup>14</sup>CO<sub>2</sub> decreased during the study period from 101.80 ± 0.47 %modern in 2017 down to 100.1 ± 0.46 %modern in 2021 (Table 1). CO<sub>2</sub> respired from the Uddjaure peat had a higher <sup>14</sup>C signature than the bulk peat (Table 1).

**Table 1. Radiocarbon activity of bulk and respired Uddjaure peat and activity of three air samples collected in 2017, 2018 and 2021.**

Publication Code <sup>1</sup>	Sample Identifier	%Modern ± 1 σ	Radiocarbon Age (years BP) ± 1 σ	CO <sub>2</sub> volume (ml)	δ <sup>13</sup> C-VPDB‰
SUERC-75755	Uddjaure bulk peat	71.41±0.33	2704±37	49.3	-27.8
SUERC-77510	Respired CO <sub>2</sub> from Uddjaure peat	78.65±0.36	1929±37	5.67	-26.7
SUERC-76444	Abisko air 2017	101.8±0.47	n/a	6.34	-8.1
SUERC-83429	Abisko air 2018	101.1±0.46	n/a	13.63	-8.8
SUERC-102436	Abisko air 2021	100.1±0.46	n/a	12.03	-9.0

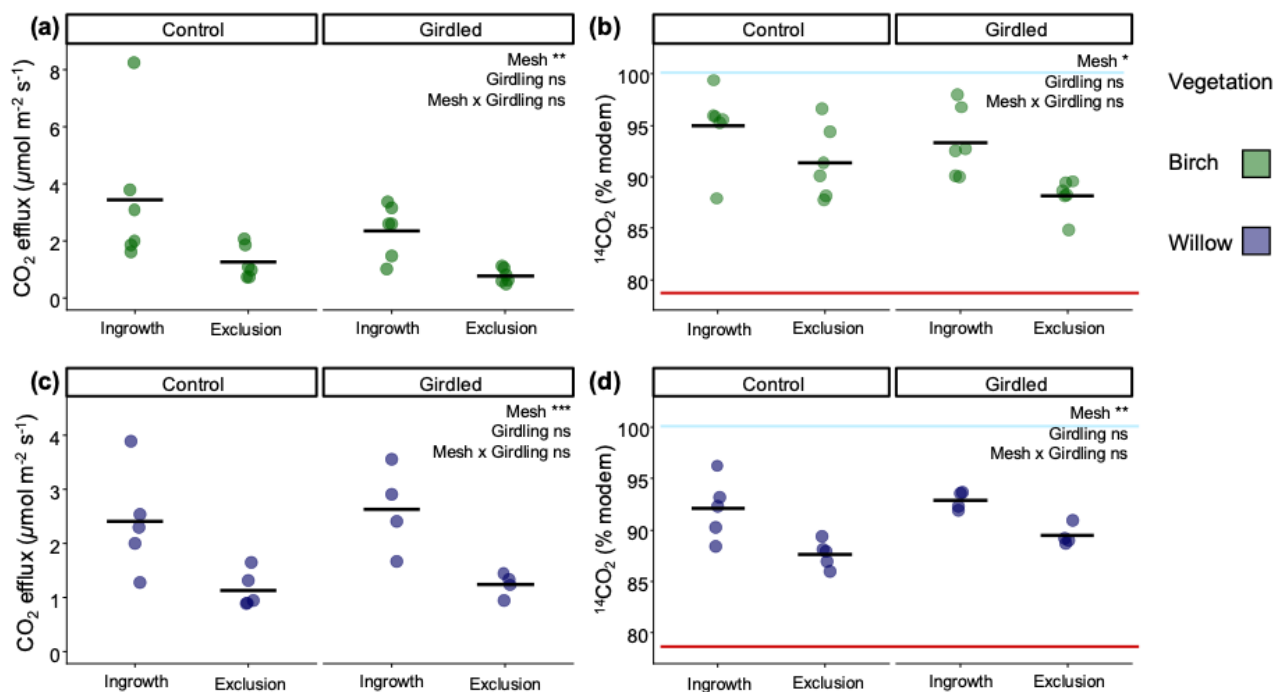
<sup>1</sup>Each radiocarbon determination receives a unique publication code

### 3.2 Root biomass, total CO<sub>2</sub> fluxes and <sup>14</sup>C content

CO<sub>2</sub> fluxes were consistently higher in the ingrowth cores relative to exclusion cores, in both control and girdling treatments. In the control plots, ingrowth cores had, on average, 64% higher CO<sub>2</sub> efflux in birch (p = 0.002) and 53% higher efflux in willow (p = 0.001) compared to exclusion cores (Fig. 2a & c). Girdling did not have a significant effect on total CO<sub>2</sub> efflux rates from the extracted cores in either birch (p = 0.15) or willow (p = 0.62). CO<sub>2</sub> fluxes from both ingrowth and exclusion peat cores were enriched in <sup>14</sup>C relative to CO<sub>2</sub> respired from Uddjaure peat under laboratory conditions (Fig. 2b & d). Slightly more enriched <sup>14</sup>CO<sub>2</sub> signatures were observed in respiration from peat cores in girdled plots, compared with ungirdled



controls, although these were neither significant in birch ( $p = 0.104$ ) nor in willow ( $p = 0.172$ ) (Fig. 2b & d; Table B1).  $^{14}\text{CO}_2$  signatures were also enriched by 5.3% modern on average in the birch ingrowth cores ( $p = 0.005$ , Fig. 2b) and enriched by 7.7% modern in the willow ingrowth cores ( $p = 0.001$ , Fig. 2d) relative to the exclusion cores in the control treatments (Fig. 2b-d; Table B1). No significant interactions were found between the presence or absence of roots and the girdling treatment for either total  $\text{CO}_2$  efflux or  $^{14}\text{C}$  content (Table B1). Root biomass was higher in the ingrowth cores than in exclusion cores ( $p < 0.001$ ) across both vegetation types, confirming the effectiveness of the exclusion mesh treatment within plots (Fig B2; Table B2). However, there was no significant effect of the girdling treatment on root biomass across all vegetation types ( $p = 0.755$ ; Fig B2; Table B2).

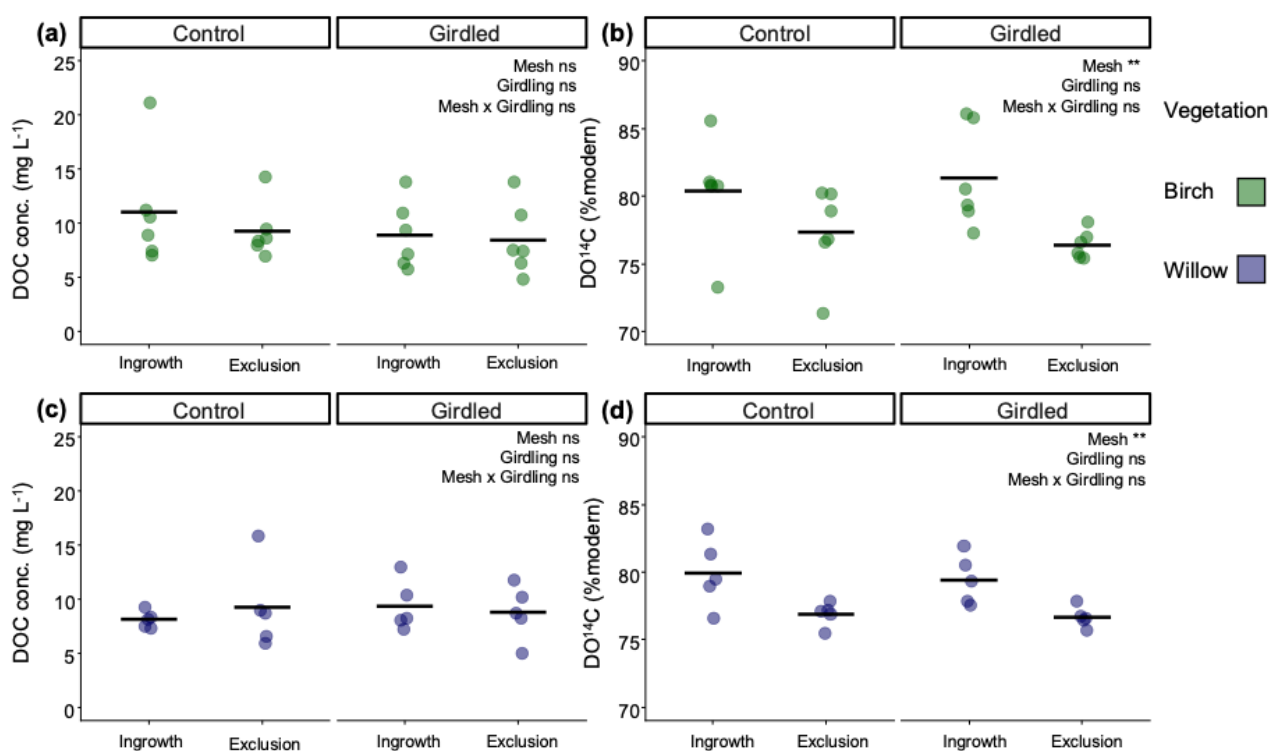


270 **Figure 2a-d.  $\text{CO}_2$  effluxes and  $^{14}\text{C}$  content of respiration from peat cores.** Individual points and means for total  $\text{CO}_2$  efflux ( $\mu\text{mol m}^{-2} \text{s}^{-1}$ ) (a & c) and  $^{14}\text{CO}_2$  signature (%modern) (b & d) for peat cores in birch control treatment ( $n=6$ ) and girdled treatment ( $n=6$ ) and willow control treatment ( $n=5$ ) and girdled treatment ( $n=4$ ). Peat cores (abbr. Ingrowth = 2-mm mesh and Exclusion = 1- $\mu\text{m}$  mesh) are presented on the x-axis. Individual points are randomly spaced along the x-axis. Mean values are represented by horizontal black bars. Significance of fixed effects in linear mixed effects models indicated as:  
 275 \*\*\*  $p < 0.001$ , \*\*  $p < 0.01$ , \*  $p < 0.05$ , ns = non-significant (Table B1). The solid horizontal lines in b) and d) represent the  $^{14}\text{C}$  content of atmospheric  $\text{CO}_2$  (blue) and pure peat-derived  $\text{CO}_2$  under laboratory incubation (red).



### 3.3 Soil DOC concentrations and $^{14}\text{C}$ content

280 Extracted DOC concentrations were similar across treatments, with no significant effects of either girdling, rhizosphere exclusion or their interaction (Fig. 3a&c; Table B3). However,  $\text{DO}^{14}\text{C}$  signatures were significantly more enriched in ingrowth cores relative to exclusion cores, in both birch ( $p = 0.009$ ) and willow ( $p = 0.006$ ) (Fig. 3b&d; Table B3). There was no significant difference in the average  $^{14}\text{C}$  content of DOC between girdled and control treatments and no significant interaction between girdling and core type (Table B3).



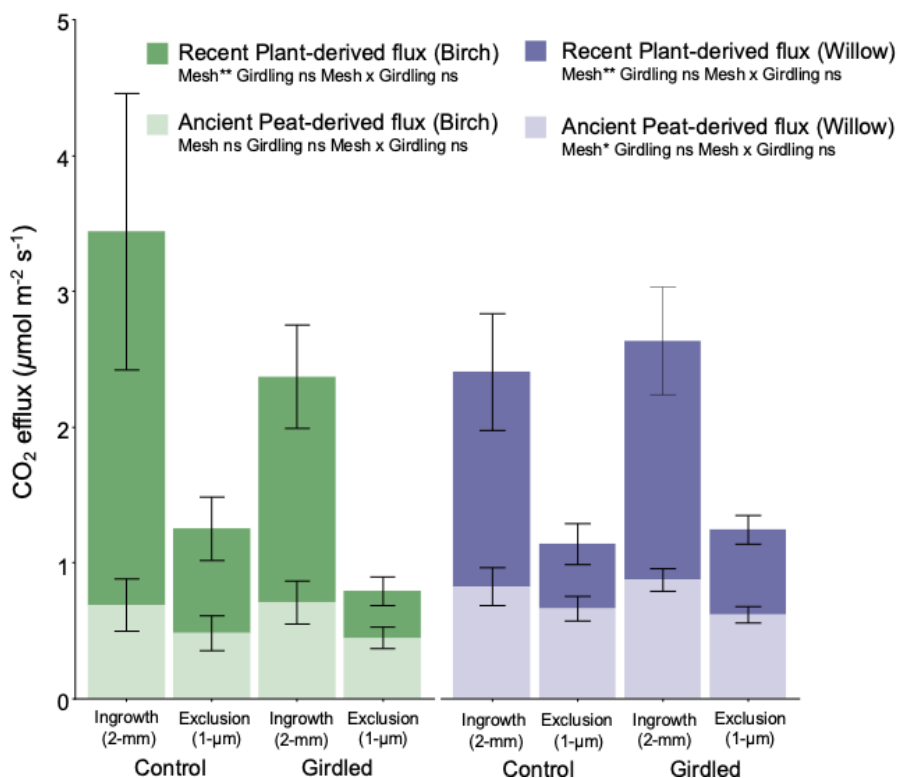
285

290 **Figure 3a-d. DOC concentrations and radiocarbon signatures from ingrowth soil cores.** Individual points and means of  $\text{DO}^{14}\text{C}$  signature (%modern) and soil DOC concentrations ( $\text{mg L}^{-1}$ ) of peat cores (abbr. Ingrowth = 2-mm mesh and Exclusion = 1- $\mu\text{m}$  mesh) in birch girdled ( $n = 6, 6$ ) and control ( $n = 5, 5$ ) plots and willow control ( $n = 5, 5$ ) and girdled ( $n = 5, 5$ ) plots. Significance of fixed effects in linear mixed effects models indicated as: \*\*\*  $p < 0.001$ , \*\*  $p < 0.01$ , \*  $p < 0.05$ , ns = non-significant (Table B4).



### 3.3 Partitioned CO<sub>2</sub> fluxes and rhizosphere priming effects

There was a significant impact of mesh size (i.e. ingrowth/exclusion) on the efflux of recent plant-derived C from the excavated  
 295 peat cores in both birch ( $p = 0.002$ ) and willow ( $p = 0.002$ ; Fig 4, Table B1). In both vegetation types, a non-significant  
 decrease in plant-derived CO<sub>2</sub> flux was found with girdling ( $p = 0.063$  and  $p = 0.276$ , for birch and willow, respectively). Even  
 where the rhizosphere was excluded, however, the modelled contribution of plant-derived carbon to the total CO<sub>2</sub> flux was  
 evident. In the exclusion mesh cores, the average recent plant-derived component was 41 – 59% of the total flux, compared to  
 63 – 76% on average for ingrowth cores (Fig 4). Differences in the modelled ancient peat-derived CO<sub>2</sub> flux were less clear  
 300 than the plant-derived flux in birch, as there was no statistically significant effect of mesh size ( $p = 0.538$ ) or girdling treatment  
 ( $p = 0.954$ ). Willow, in contrast, had significantly higher ancient peat-derived fluxes from ingrowth cores than from exclusion  
 cores ( $p = 0.046$ ), while girdling caused no significant effect on the ancient peat-derived flux ( $p = 0.768$ , Fig 4. Table B1).



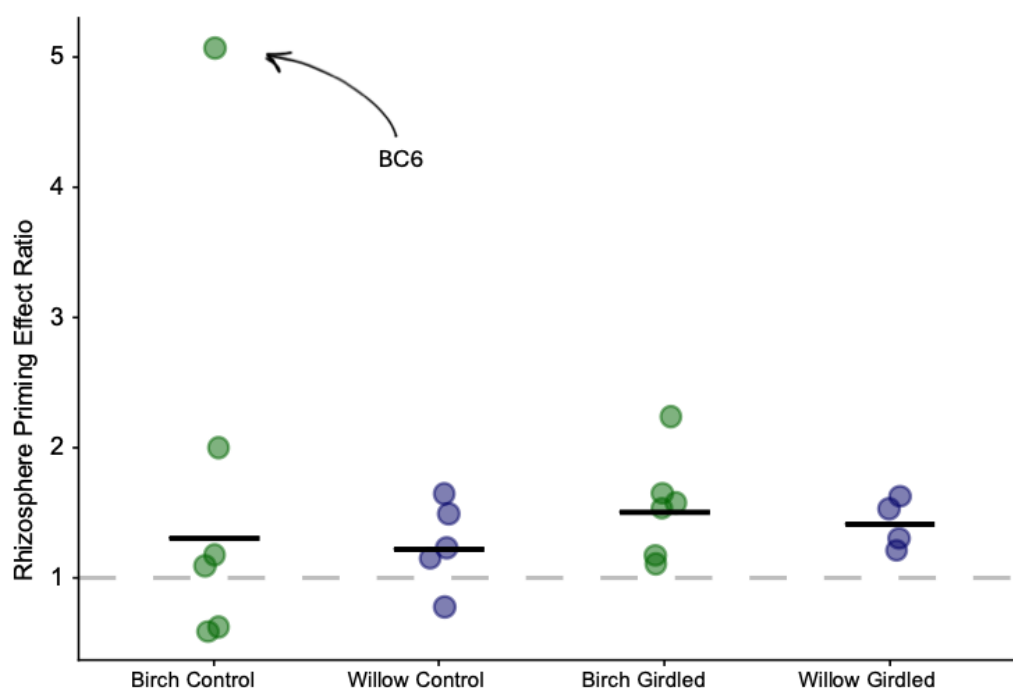
305 **Figure 4. Partitioned (modelled) CO<sub>2</sub> fluxes for each vegetation type and treatment.** Modelled recent plant-derived CO<sub>2</sub>  
 flux and ancient peat-derived CO<sub>2</sub> flux in control and girdled treatments in birch and willow vegetation based on source  
 partitioning using natural abundance radiocarbon signatures of sources. Significance of fixed effects in linear mixed effects  
 models are indicated as: \*\*\*  $p < 0.001$ , \*\*  $p < 0.01$ , \*  $p < 0.05$ , ns = non-significant (Table B1). Error bars represent the  
 standard errors of the means.



310

Generally, rhizosphere priming effect (RPE) ratios were  $> 1$  (Fig. 5), meaning that peat-derived  $\text{CO}_2$  fluxes were higher from the ingrowth cores than from the paired exclusion cores, consistent with positive priming. One plot (BC6; birch control #6) had a notably high total  $\text{CO}_2$  flux (Fig. 2) which also translated to a notably high RPE value (Fig. 5). When all data were included (there was no analytical justification for removal of BC6) the RPE ratios were significantly  $> 1$  ( $p = 0.01$ ). This effect was still maintained even when BC6 was excluded from the analysis ( $p = 0.005$ ; Table B4). There was, however, no statistically significant effect of either vegetation ( $p = 0.764$ ) or girdling treatment ( $p = 0.507$ ) on the RPE ratio (Table B4), even though the average across all groups was 1.36; on average the peat-derived  $\text{CO}_2$  flux was 36% higher in ingrowth cores than in exclusion cores.

315



320 **Figure 5. Rhizosphere priming effect (RPE) ratios for each vegetation type and treatment.** The rhizosphere priming effect ratio was calculated using Equation 5 where the ancient peat-derived flux in ingrowth cores was divided by the ancient peat-derived flux in the paired exclusion cores. Horizontal lines indicate mean values (after taking the exponent of the mean of the natural log transformed RPE ratios). Birch control #6 (BC6) had a notably high total  $\text{CO}_2$  flux but was not excluded from the analysis.

325

Consistent with earlier ecosystem ecology publications using atmospheric natural abundance  $^{14}\text{C}$  signatures (see Gavazov et al. (2018) and references therein) our modelling assumed contemporary (in this case, 2021) atmospheric  $^{14}\text{C}$  abundance ( $\Delta_{air}$ ;



Eq. 2) in autotrophic belowground fluxes (Table 1). Our analysis (Appendix B) confirmed that our conclusions on RPEs were robust regardless of whether we used current year (2021) atmospheric  $^{14}\text{C}$  values or those from the first year of girdling (2017).

#### 330 4 Discussion

We experimentally controlled the access of roots to peat cores deployed *in situ* in two treeline ecotone vegetation types over a four-year period using meshes of two contrasting sizes. The  $^{14}\text{C}$  content of respired  $\text{CO}_2$  allowed the partitioning of fluxes from recently-fixed (root, mycorrhizal and potentially also litter sources) *versus* ancient peat-derived sources. As expected, where roots were excluded, the recent plant-derived component of respiration was significantly reduced. Differences in the  
335 peat-derived component of respiration between the rooted and non-rooted cores revealed impacts of roots and associated biota on rates of decomposition; the clearest test yet of rhizosphere priming under field conditions. The overall positive rhizosphere priming effect (RPE) of ~36% (based on mesh-size comparison) was statistically significant, while neither vegetation type nor girdling treatment, nor their interactions, were influential. There was generally a positive, and statistically significant, effect of roots and associated soil organisms on respiration from peat, consistent with positive priming, but the response was variable,  
340 with examples ranging from very high positive (BC6), through neutral, to some (4 out of 21 pairs) negative priming effects. These results are consistent with growing evidence, underpinned by advances in rhizosphere imaging and isotope techniques (Becker and Holz, 2021; Denis et al., 2019), of rhizosphere priming occurring as ‘hotspots’ and ‘hot moments’ in soils. These are indicative of strong spatial and temporal heterogeneity in soil microbial activity (Kuzyakov and Blagodatskaya, 2015) often linked to input of labile organic compounds by plants, both above- and belowground.

345 Our approach clearly demonstrates that soil respiration fluxes can be partitioned based on distinct  $^{14}\text{C}$  signatures of the substrate and recent plant-derived inputs. Although a high contribution of root-derived carbon to this flux was expected, there was also an important contribution of recently fixed C to respiration and DOC concentrations in the absence of roots. The modelled plant-derived, recently assimilated C made a significant contribution to  $\text{CO}_2$  fluxes and to DOC, even for peat cores where  
350 roots had been excluded. This finding suggests that relatively  $^{14}\text{C}$ -enriched C was entering the 1- $\mu\text{m}$  cores and being metabolised, possibly through leaching of DOC from above and the surrounding soil, or possibly also via ingrowth of very fine hyphae, with subsequent proliferation inside the cores. Autotrophic inputs via leaching of litter, moss establishment and germinating seedlings could be further minimized in future studies. Nevertheless, our approach was successful in manipulating the input of recent plant-derived C into peat via roots.

355 The difference in modelled peat-derived respiration in the rooted and unrooted cores allowed us to calculate an average rhizosphere priming effect of ca. 1.36 across all vegetation and treatment types, marking the first quantification of this effect *in situ* in natural vegetation communities. By contrast, most studies to date have involved lab incubations, commonly adding  $^{13}\text{C}$ -labelled compounds such as cellulose, glucose, proteins, amino acids, or other simple compounds, to sieved soils in the



360 absence of roots or mycorrhizal fungi (Wild et al., 2016; Wild et al., 2023; Hicks et al., 2020). In a further development,  
Friggens et al. (2025) grew non-native plants in tundra soils under controlled conditions. These studies, with their tight  
environmental control, and also in combination with modelling approaches (Keuper et al., 2020), provide valuable insights,  
while our approach is complementary, offering a new perspective and marking a significant step forward in understanding  
priming under field conditions. Indeed, in a recent analysis of laboratory experiments where  $^{13}\text{C}$ -labelled substrates were added  
365 to permafrost peat soils (Wild et al., 2023), organic soils were unresponsive (with a relative RPE of  $\sim 1$ ) to labile carbon  
addition, whereas mineral permafrost soils showed a positive priming effect (RPE  $> 1$ ). Likewise, Friggens et al. (2025) showed  
that the greatest RPE in response to planting with non-native grasses was observable in mineral permafrost soils. In the current  
study, however, by integrating the biological and environmental complexity associated with exposing organic substrate (peat)  
to root and rhizosphere processes *in situ* over 4 years, our data suggest that high positive priming rates are possible in tundra  
370 and treeline vegetation, but that the local response may be highly variable.

High variability in RPEs could be attributable to spatially and temporally heterogeneous soil processes across the treeline  
ecotone. In our previous work in these stands, we found that soil respiration, and mycelium and root production were highly  
variable between the ungirdled plots (Parker et al., 2020), as was the ectomycorrhizal fungal community composition (Parker  
375 et al., 2022). Indeed, Packard et al. (2025) found that fungal community composition and enzyme activity varies at small  
scales, from 10 to 1000 cm. Furthermore, saprotrophs and mycorrhizal fungi exhibit distinct vertical niche differentiation  
(Rosling et al., 2003), and ectomycorrhizal species may even associate with roots at different depths than those at which they  
produce their extramatrical mycelium (Genney et al., 2006). Therefore, high measured RPEs at specific sites (e.g. RPE = 5.07,  
plot B6C, Fig. 5) could reflect areas of high root and ectomycorrhizal activity. Equally, it has been suggested that ericoid  
380 mycorrhizal (ERM) shrubs and fungi inhibit decomposition (Clemmensen et al., 2015) and therefore drive a negative RPE via  
inhibition of saprotrophic (Fanin et al., 2022) or ectomycorrhizal decomposers (Mielke et al., 2025). We could not control the  
species composition of root ingrowth into the cores, however, so the community-level mean RPE may integrate both positive  
and negative effects associated with different organisms.

385 Contrary to our expectations, there was no significant effect of the girdling treatment on root biomass across both vegetation  
types (Fig B2; Table B2) in 2021. This may be linked with the duration of the experiment, with compensatory development of  
the understory rhizosphere in girdled plots over four growing seasons. If so, then this was an unintended artifact of the  
experiment, which ran for four, as opposed to the planned three, growing seasons. In terms of rhizosphere development in the  
cores compared with surrounding undisturbed soils, the work of Sloan et al. (2013) makes it possible to make direct  
390 comparisons, but only for willow communities. Mean root biomass in the ingrowth cores varied from  $51.1 \pm 15.1$  to  $48.8 \pm$   
 $32.7 \text{ g C m}^{-2}$  in control and girdled willow plots, respectively, which is  $\sim 7$  times lower than standing root biomass C in natural  
systems ( $\sim 350 \text{ g C m}^{-2}$  in tall *Salix* plots at Abisko (Sloan et al., 2013)). Standing root biomass in our cores in the control birch  
plots was likely also much lower than in the natural system, although Sloan et al. (2013) do not provide data for natural birch



forest at Abisko. Therefore, there may have been scope in our methods to enhance root and hyphal ingrowth relative to peat  
395 volume, to improve the robustness of our RPE estimates as well as to aid in identifying roots to species or functional types. A  
research priority should thus be to strengthen the interaction between  $^{14}\text{C}$ - depleted peat and root and rhizosphere processes to  
the point where root production and activity, as well as microbial interactions (e.g. competition between ectomycorrhizas and  
saprotrophs), better reflect the natural environment. Although we have measured significant RPEs in the field, there is scope  
for further method development to tackle spatial and temporal variability in RPEs and the underpinning biological processes.  
400 We further acknowledge that, four years after implementation, our girdling treatment was likely beyond peak effectiveness for  
 $\text{CO}_2$  and DOC sampling, due to substantial above-ground die-back of the canopy-forming birch and willow.

Given that ECM fungi are understood to be the primary driver of late-stage decomposition in treeline subarctic (Clemmensen  
et al., 2021) and boreal forests (Sterkenburg et al., 2018), we expected that girdling of the canopy-forming ectomycorrhizal  
405 hosts would cause a reduction in positive priming. Contrary to our expectations, however, we measured similar priming in  
control plots and their girdled counterparts (Fig. 5, Table B4). Furthermore, neither root ingrowth into the 2-mm mesh cores,  
nor the relative contribution of recently assimilated plant C to respiration fluxes differed significantly between control and  
girdled plots (Table B2, Fig. B2). In the first two growing seasons post-girdling (2017 and 2018), peak growing season soil  
respiration was reduced substantially, by 46-53% and 30-38% in birch and willow plots, respectively (Parker et al., 2020).  
410 Much of the reduction was likely the result of cessation of birch and willow root respiration, as expected, suggesting that the  
decrease in root growth observed in the initial years of the experiment (Parker et al., 2020) might have been compensated for  
in subsequent growing seasons by production from the ericaceous and herbaceous understorey. Compensatory root growth by  
the ericaceous understorey may also have explained the lack of a significant girdling effect on priming (Table B4), thus leading  
us to underestimate the girdling effect, although this challenges assumptions about the relative roles of ERM and ECM fungi  
415 in priming. ERM fungi are a guild with a diverse range of genes coding for nutrient acquisition from organic sources (Martino  
et al., 2018) and despite our initial hypotheses, understorey plants also appear to be responsible for priming. Indeed, work by  
Grelet et al. (2009) suggests that some ERM fungi can also form ECM, and the niche separation of ERM and ECM hosts may  
be less clear-cut than is often assumed.

420 The approach of utilising the natural abundance  $^{14}\text{C}$  content of an ancient  $^{14}\text{C}$ -depleted peat soil as a distinct tracer to estimate  
priming effects *in situ* could have wide applicability across systems. Although peat soils only cover 3-4% of the Earth's  
terrestrial surface, they store up to 30% of soil C; thus, the preservation of peat, for this and many other reasons, is critically  
important (Unep, 2022), but see also Cr  z   et al. (2025). In circumstances where peat has been afforested (Sloan et al., 2019;  
Defrenne et al., 2023), or converted to grassland or agriculture (Hutchinson, 1980), it is challenging to distinguishing C losses  
425 due to rhizosphere processes from those caused directly by drainage and thus changes in oxygen and redox potential (Evans  
et al., 2021). However, such converted and managed systems may exhibit less heterogeneity than those we studied here,  
potentially rendering our method more powerful in these contexts. Indeed, priming is hypothesised as a mechanism for C loss



when trees are planted on temperate ericaceous organic soils (Friggens et al., 2020), and it may have an important role in destabilisation and loss of organic matter following afforestation of peatlands. Equally, peat is being mobilised from eroding systems around the world and deposited downstream, in systems where roots of productive plants may exert a strong priming effect, enhance decomposition rates and impact on GHG budgets for peatlands (Parker et al., 2025). Plant productivity in the subarctic landscape studied here is strongly limited by low temperature, low soil fertility and short growing season length. We therefore suggest that if our method were deployed in more productive temperate soils, RPEs could be identified and quantified with more confidence due to a potentially more active mycorrhizosphere and root-associated soil biota showing more rapid exploration of the test substrates. However, to obtain a reliable radiocarbon contrast between SOM and contemporary C inputs to the rhizosphere requires organic substrates of significant age (i.e.  $^{14}\text{C}$  depletion) to accommodate continued reduction in atmospheric isotopic enrichment via the Suess Effect (Michaud et al., 2024). We also want to emphasize that we deployed just one boreal peat substrate here, where there were substantial age contrasts between bulk peat and respired  $\text{CO}_2$  (Table 1). We therefore acknowledge that the substrate itself is heterogeneous, and there might be shifts in the lability and  $^{14}\text{C}$  age of organic matter being primed through the duration of the experiment, potentially further interacting with microbial hotspots or hot moments. Our approach, nonetheless, gives a fourth year ‘snap-shot’ of the potential for priming in two contrasting systems (indeed four, including girdled plots), which was notably consistent given the high variability around the mean values (Fig. 5). We are also confident that our set-up also holds particular promise in the context of thawing of permafrost and thermokarst exposure of previously unrooted, ancient, material exposed to new root activity.

445

In conclusion, we show that it is possible to partition soil respiration into recent and ancient sources based on the use of natural abundance  $^{14}\text{CO}_2$  produced from peat ingrowth cores *in situ*. Based on the partitioning calculations, and by comparing cores that allow or restrict root ingrowth, it is further possible to estimate RPEs in the field. We found predominantly positive priming ( $p = 0.01$ ) of the ancient peat substrate across mountain birch forest and woolly willow stands, even after girdling. However, there was also substantial variability, potentially consistent with the existence of microbial ‘hotspots and moments’. By contrast, we could not identify any statistically significant contrasts in RPEs between the two vegetation communities, nor any effect of girdling. For the latter, it is possible that compensatory rhizosphere development by the understorey plants reduced the importance of C supply by the canopy-forming species. Overall, our unique experimental approach, deployed for the first time *in situ* within natural communities, has successfully identified positive rhizosphere priming. Our evaluation of the approach highlights optimisations that can be made to better represent the natural system (e.g. encouraging more representative and extensive root ingrowth, in addition to identifying root and microbial communities) but demonstrates transformative progress toward a more robust quantification and exemplification of RPEs. Our study underscores the pivotal role of rhizosphere processes and plant-microbe-soil interactions for understanding how recently assimilated C interacts with SOM to determine whole-ecosystem C dynamics.

460

## Appendix A

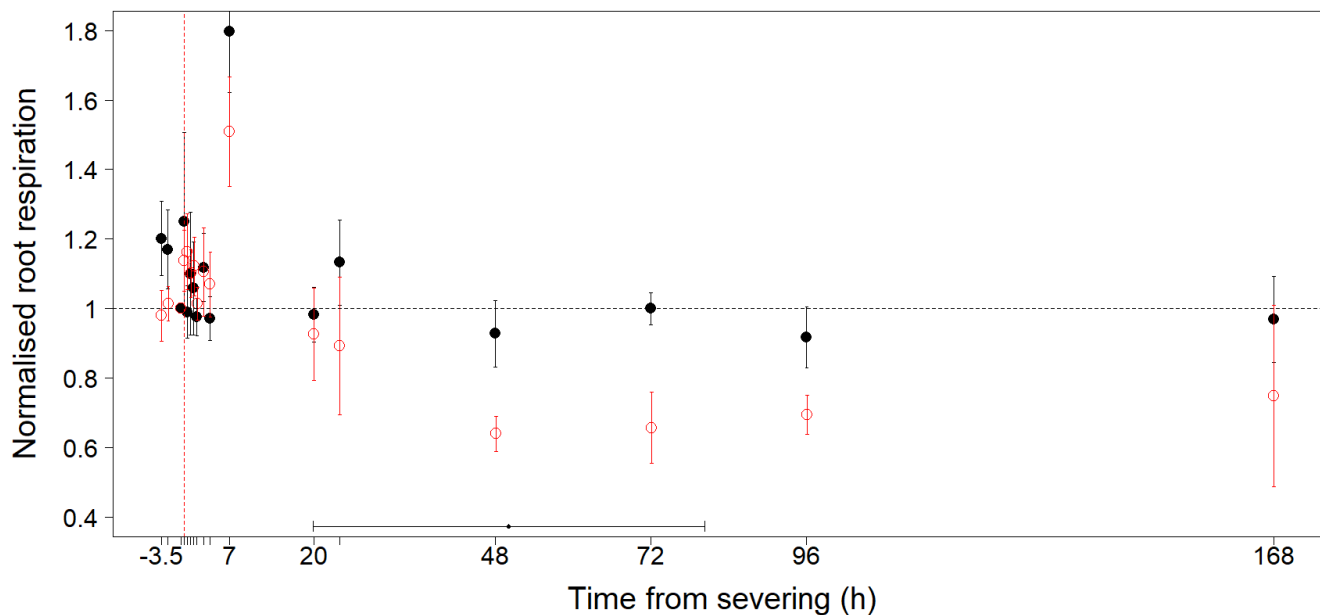


### *Root severing experiment*

465 Continued root and mycorrhizal activity in the ingrowth cores during respiration measurement and CO<sub>2</sub> collection is a  
key assumption of our severing and CO<sub>2</sub> collection approach. We tested this assumption in a birch (*Betula pendula*) forest in  
Stirling, UK. On 15<sup>th</sup> October 2020, birch roots in the upper 20 cm of soil over an area of ~20 x 20 cm, all connected to a  
single coarse root were excavated. All roots were washed then repacked into a 14 x 7 x 10 cm plastic box with washed quartz  
up to 7 cm (leaving 3 cm head space), and the root system laid halfway at 3.5 cm depth. As the boxes contained sand and no  
470 organic matter, 3-4 slow-release nutrient pellets were mixed in to encourage root growth. The boxes had a 3.5 cm slot cut from  
the top to pass the live coarse root through; once inserted, the rest of the slot was then filled with non-setting putty (Evo-Stik  
Plumber's Mait) to ensure the box was airtight when the lid was sealed. After installing boxes, lids were loosely placed on top  
of each box to prevent flooding, and roots were allowed to grow into the sand matrix for 8 months. Boxes were watered as  
needed. Replicated boxes were placed in spatial blocks of two with the intention of severing one; however, some of the root  
475 systems died, leaving 6 that could be severed and 7 non-severed control plots, without direct pairing possible. Three boxes  
were placed in the soil in the same way as the rooted boxes but without any roots, acting as an un-rooted control.

On 28 June 2021, the root system in six of the boxes was severed from the tree by cutting the single coarse root that fed  
into the box. Root respiration was measured by sealing the box and measuring the increase in [CO<sub>2</sub>] over a 100 second period  
using a PP Systems EGM-5 infra-red gas analyser. Measurements were taken 4, 3.5, 2.5 and 0.5 h before severing, then at the  
480 time of severing, and again at 0.5, 1, 1.5, 2, 3, 4, 7, 20, 24, 48, 72, 96 and 168 h after severing. After these measurements, all  
roots were harvested, split into fine root and coarse roots based on a 2-mm diameter threshold, dried at 70°C for 48 h and  
weighed. Fluxes were normalised by weight of fine roots and the root respiration in each box 0.5 h before the severing  
treatment. The time post severing at which root respiration (per g fine root) changed in the severed cores was estimated by  
segmented regression analysis in the R package 'segmented' (Muggeo 2008).

485 We determined, from this separate experiment, that root severing had no effect on root respiration rates until after 50  
hours ( $P < 0.001$ ; Figure A1) while there was no clear breakpoint in the controls ( $P = 0.104$ ). Therefore, we can reasonably  
conclude that root and mycorrhizal respiration was unaltered during the CO<sub>2</sub> collections shortly after severing in the main  
experiment at the subarctic sites.



490 **Figure A1. Hourly time series of normalised birch root respiration since time from severing.** The y-intercepts reflect  
the root CO<sub>2</sub> efflux ( $\mu\text{mol s}^{-1}$ ) normalised by the grams of fine roots in the absence of other sources and is used to assess the  
longevity of the roots over time (x-axis in hours). Control roots (uncut) are displayed in black and cut roots are open red  
circles. The segmented regression analysis (see source code) found an inflection point at 50 hours ( $\pm 1$  SE (marked with  
horizontal error bar)).

495



## Appendix B

### 500 Keeling plot

In the instance of atmospheric contamination (ingress) of headspace CO<sub>2</sub>, radiocarbon results are sensitive to the  $\delta^{13}\text{C}$  value chosen for the atmospheric correction; however, there is a strong *a priori* reason to expect small but systematic differences in  $\delta^{13}\text{CO}_2$  in respiration from the rooted peat cores compared to the heterotroph peat cores, given there is a large autotrophic component to the flux in the rooted peat cores. Therefore, the y- intercepts from Keeling plots of root-derived (2-mm mesh) and heterotroph (1- $\mu\text{m}$ ) derived peat cores (Fig. B1;  $-25.5\text{‰}$  for the heterotroph correction, and  $-28.8\text{‰}$  for the rooted correction) were used as  $\delta^{13}\text{C}_{resp}$  to inform the fraction of atmospheric contamination for all samples in Equation 1.

510

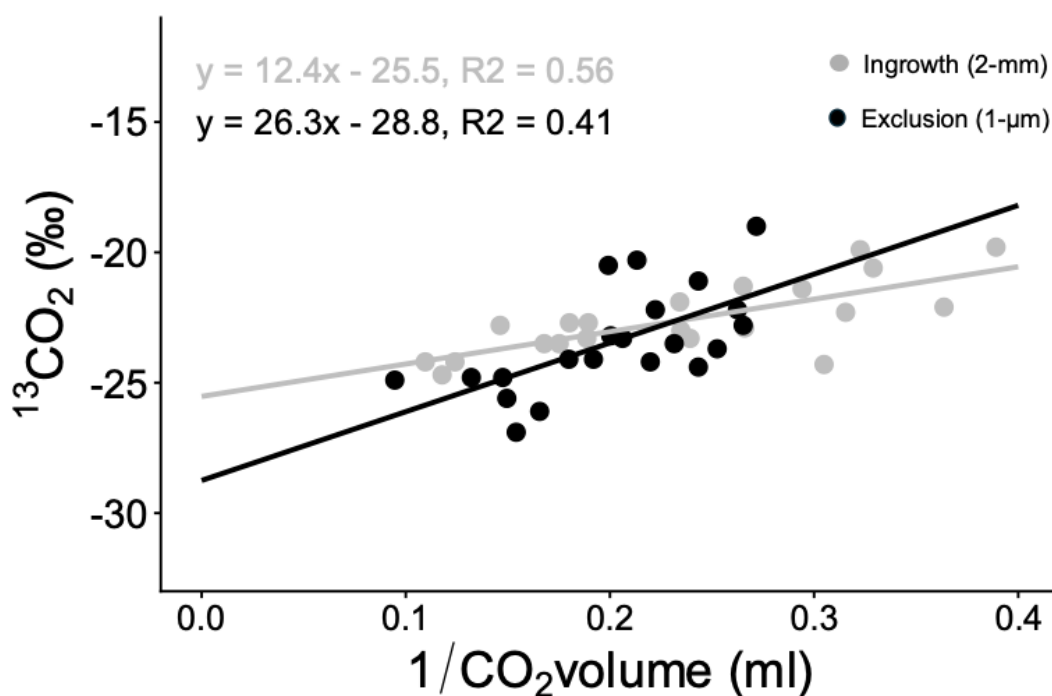


**Figure B1. Keeling plots of CO<sub>2</sub> collected on molecular sieve cartridges demonstrate the  $\delta^{13}\text{CO}_2$  versus 1/ volume of sample collected.** The y-intercepts reflect the  $\delta^{13}\text{CO}_2$  of respiration ( $\delta^{13}\text{C}_{resp}$ ) in the absence of other sources and are used to correct the  $^{14}\text{CO}_2$  data for atmospheric contamination.

515

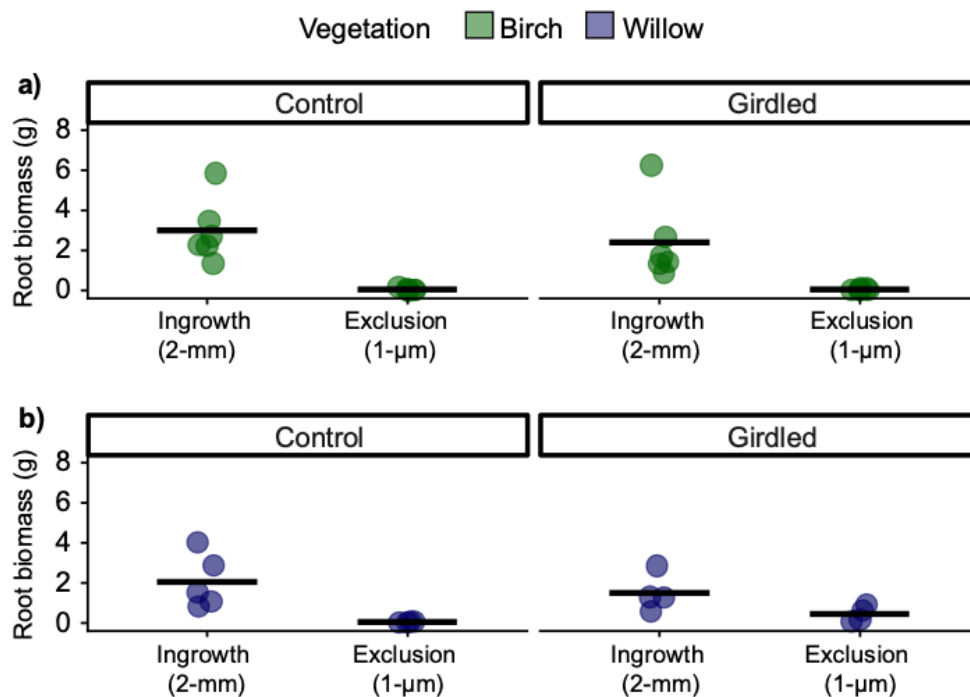


**Figure B2 Root biomass in cores with windows of different mesh sizes for each vegetation type and treatment.**

520 Individual points and means for root biomass (g) from soil cores in birch control (n=6,6), birch girdled (n=6,6) and willow control (n=5,6; blue) and willow girdled (n=4,4) plots for ingrowth and exclusion peat mesh cores), respectively. Individual points are randomly spaced along the x-axis.



525 **Table B1.** Linear mixed effects model output from the total soil CO<sub>2</sub> efflux (μmol m<sup>-2</sup> s<sup>-1</sup>), <sup>14</sup>CO<sub>2</sub> signature (%modern), modelled recent plant-derived CO<sub>2</sub> flux (μmol m<sup>-2</sup> s<sup>-1</sup>) and modelled ancient peat-derived CO<sub>2</sub> flux (μmol m<sup>-2</sup> s<sup>-1</sup>) from peat cores in girdled and control plots within birch and willow vegetation based on the atmospheric <sup>14</sup>CO<sub>2</sub> signature from the time of sampling (2021). Mesh (2-mm) refers to ingrowth peat cores.

**Birch**

log(CO <sub>2</sub> efflux μmol m <sup>-2</sup> s <sup>-1</sup> )	Estimate	Std. Error	DF	t-value	p-value
(Intercept)	0.139	0.193	10	0.721	0.487
Mesh (2-mm)	0.923	0.221	10	4.173	0.002 **
Treatment (Girdled)	-0.422	0.274	10	-1.541	0.154
Mesh (2-mm) x Treatment (Girdled)	0.139	0.313	10	0.445	0.666

log( <sup>14</sup> CO <sub>2</sub> ‰)	Estimate	Std. Error	DF	t-value	p-value
(Intercept)	4.515	0.014	10	319.333	0
Mesh (2-mm)	0.038	0.015	10	2.572	0.028 *
Treatment (Girdled)	-0.036	0.02	10	-1.787	0.104
Mesh (2-mm) x Treatment (Girdled)	0.019	0.021	10	0.879	0.4

Recent plant-derived log(CO <sub>2</sub> efflux μmol m <sup>-2</sup> s <sup>-1</sup> )	Estimate	Std. Error	DF	t-value	p-value
(Intercept)	-0.412	0.238	10	-1.734	0.114
Mesh (2-mm)	1.178	0.283	10	4.16	0.002 **
Treatment (Girdled)	-0.712	0.336	10	-2.118	0.06
Mesh (2-mm) x Treatment (Girdled)	0.326	0.4	10	0.814	0.434

Ancient peat-derived log(CO <sub>2</sub> efflux μmol m <sup>-2</sup> s <sup>-1</sup> )	Estimate	Std. Error	DF	t-value	p-value
(Intercept)	-0.85	0.267	10	-3.185	0.01
Mesh (2-mm)	0.172	0.269	10	0.638	0.538
Treatment (Girdled)	-0.022	0.377	10	-0.06	0.954
Mesh (2-mm) x Treatment (Girdled)	0.177	0.381	10	0.464	0.652

**Willow**

log(CO <sub>2</sub> efflux μmol m <sup>-2</sup> s <sup>-1</sup> )	Estimate	Std. Error	DF	t-value	p-value
(Intercept)	0.097	0.139	7	0.7	0.507
Mesh (2-mm)	0.716	0.126	7	5.663	0.001 ***
Treatment (Girdled)	0.108	0.209	7	0.519	0.62
Mesh (2-mm) x Treatment (Girdled)	0.01	0.19	7	0.052	0.96

log( <sup>14</sup> CO <sub>2</sub> ‰)	Estimate	Std. Error	DF	t-value	p-value
(Intercept)	4.473	0.009	7	490.97	0
Mesh (2-mm)	0.049	0.013	7	3.832	0.006 **
Treatment (Girdled)	0.021	0.014	7	1.521	0.172
Mesh (2-mm) x Treatment (Girdled)	-0.012	0.019	7	-0.624	0.553

Recent plant-derived log(CO <sub>2</sub> efflux μmol m <sup>-2</sup> s <sup>-1</sup> )	Estimate	Std. Error	DF	t-value	p-value
(Intercept)	-0.78	0.172	7	-4.542	0.003
Mesh (2-mm)	1.113	0.222	7	5.022	0.002 **
Treatment (Girdled)	0.305	0.258	7	1.183	0.276
Mesh (2-mm) x Treatment (Girdled)	-0.111	0.332	7	-0.335	0.747

Ancient peat-derived log(CO <sub>2</sub> efflux μmol m <sup>-2</sup> s <sup>-1</sup> )	Estimate	Std. Error	DF	t-value	p-value
(Intercept)	-0.452	0.129	7	-3.509	0.01
Mesh (2-mm)	0.223	0.092	7	2.423	0.046 *
Treatment (Girdled)	-0.059	0.193	7	-0.307	0.768
Mesh (2-mm) x Treatment (Girdled)	0.105	0.138	7	0.762	0.471

530

**Table B2.** Linear mixed model of mesh and girdling treatment effects on root biomass across both vegetation types.

log(Root biomass (g))	Estimate	Std. Error	DF	t-value	p-value
(Intercept)	0.605	0.049	19	12.444	0
Mesh (2-mm)	-0.497	0.049	19	-10.23	< 0.001 ***
Treatment (Girdled)	0.015	0.049	19	0.317	0.755
Mesh (2-mm) x Treatment (Girdled)	-0.077	0.049	19	-1.582	0.13

535

**Table B3.** Linear mixed effects model output from the soil DOC concentration (mg L<sup>-1</sup>) and DO<sup>14</sup>C signature (%modern) of peat cores in girdled and control plots within birch and willow vegetation. Mesh (2-mm) refers to ingrowth peat cores. Significance of fixed effects in linear mixed effects models indicated as: \*\*\* p < 0.001.



### Birch

log(DOC mg L <sup>-1</sup> )	Estimate	Std. Error	DF	t-value	p-value
(Intercept)	2.198	0.142	10	15.509	0
Mesh (2-mm)	0.13	0.126	10	1.032	0.326
Treatment (Girdled)	-0.127	0.2	10	-0.635	0.54
Mesh (2-mm) x Treatment (Girdled)	-0.064	0.178	10	-0.363	0.724

### Willow

log(DOC mg L <sup>-1</sup> )	Estimate	Std. Error	DF	t-value	p-value
(Intercept)	2.159	0.126	8	17.196	0
Mesh (2-mm)	-0.066	0.173	8	-0.384	0.711
Treatment (Girdled)	-0.024	0.178	8	-0.137	0.894
Mesh (2-mm) x Treatment (Girdled)	0.146	0.245	8	0.598	0.566

log(DO <sup>14</sup> C %modern)	Estimate	Std. Error	DF	t-value	p-value
(Intercept)	4.347	0.017	10	259.799	0
Mesh (2-mm)	0.038	0.012	10	3.206	0.009 **
Treatment (Girdled)	-0.012	0.024	10	-0.493	0.632
Mesh (2-mm) x Treatment (Girdled)	0.024	0.017	10	1.412	0.188

log(DO <sup>14</sup> C %modern)	Estimate	Std. Error	DF	t-value	p-value
(Intercept)	4.342	0.009	8	464.974	0
Mesh (2-mm)	0.038	0.01	8	3.699	0.006 **
Treatment (Girdled)	-0.003	0.013	8	-0.218	0.833
Mesh (2-mm) x Treatment (Girdled)	-0.003	0.015	8	-0.195	0.85

540

**Table B4.** Linear model output for rhizosphere priming effect ratios in girdled and control plots within birch and willow vegetation including and excluding the paired plots from birch control in plot 6 (BC6). Significance of fixed effects in linear mixed effects models indicated as: \*\* p < 0.01, \* p < 0.05.

### RPE ratios

ln(log(RPE) ~ Vegetation x Treatment)	Estimate	Std. Error	t-value	p-value
(Intercept)	0.308	0.106	2.893	0.01 *
Vegetation (Birch)	0.032	0.106	0.305	0.764
Treatment (Girdling)	-0.072	0.106	-0.678	0.507
Vegetation x Treatment	-0.001	0.106	-0.007	0.995

### RPE ratios excluding BC6

ln(log(RPE) ~ Vegetation x Treatment)	Estimate	Std. Error	t-value	p-value
(Intercept)	0.24	0.074	3.241	0.005 **
Vegetation (Birch)	-0.035	0.074	-0.479	0.639
Treatment (Girdling)	-0.14	0.074	-1.892	0.077
Vegetation x Treatment	-0.069	0.074	-0.927	0.368

545

### Sensitivity Analysis of Autotrophic Belowground Fluxes to changes in Atmospheric Abundance of <sup>14</sup>C

Consistent with earlier ecosystem ecology publications using atmospheric natural abundance <sup>14</sup>C signatures (see Gavazov et al. (2018) and references therein) our modelling assumed contemporary (in this case, 2021) atmospheric <sup>14</sup>C abundance ( $\Delta_{air}$ ; Eq. 2) in autotrophic belowground fluxes (Table 1). During our study period, however, there was a modest, but measurable, decline in %modern atmospheric <sup>14</sup>CO<sub>2</sub> content between 2017 and 2021 (Table 1). Interannual and longer-term changes in atmospheric <sup>14</sup>C abundance are a consequence, among other factors, of fossil fuel CO<sub>2</sub> emissions to the atmosphere (which are heavily <sup>14</sup>C-depleted) and the atmospheric atomic weapons testing of the late 1950s and early 60s (see Fig. 3 in Graven et al. (2020)). We acknowledge the possible contribution of plant stored C to both root and shoot growth, and autotrophic respiration, because age-related differences in atmospheric <sup>14</sup>CO<sub>2</sub> activity (Table 1), and thus plant-assimilated C, could alter the modelled contributions to priming estimated from plant-derived respiration. We therefore tested this assumption, using the more enriched atmospheric <sup>14</sup>CO<sub>2</sub>,  $\Delta_{air}$  (%modern) from 2017, four years prior to peat core sample collection, as an alternative end-member to 2021. Our analysis confirmed that our conclusions on RPEs were robust regardless of whether we used current year (2021) atmospheric <sup>14</sup>C values or those from the first year of girdling (2017). In short, using the  $\Delta_{air}$  of 2017 reduced the estimated fraction of autotrophic respiration, and increased estimated positive priming compared to estimates based on  $\Delta_{air}$  from 2021.

560



### **Code and data availability**

Underlying research data and R code will be deposited and made publicly available on the University of Stirling's research repository (STORRE; <https://storre.stir.ac.uk/>) upon publication of the article.

### 565 **Supplement link**

The link to the supplement will be included by Copernicus.

### **Author contributions**

570 PW, TP, LS and J-AS conceived the ideas and designed methodology; TP, MG, DJ, J-AS and PW collected the data; LM LS and TP analysed the data; LM, LS and TP led the writing of the manuscript. All authors contributed critically to the analyses, written drafts and gave final approval for publication.

### **Competing interests**

No conflict of interest.

### 575 **Disclaimer**

“Copernicus Publications remains neutral with regard to jurisdictional claims made in the text, published maps, institutional affiliations, or any other geographical representation in this paper. While Copernicus Publications makes every effort to include appropriate place names, the final responsibility lies with the authors. Views expressed in the text are those of the authors and do not necessarily reflect the views of the publisher.”

### 580 **Acknowledgements**

We are very grateful to the staff of the Abisko Scientific Research Station (ANS) for hosting and facilitating our research. We also respectfully acknowledge the Sápmi reindeer herders, upon whose lands this research took place. We thank Ian Washbourne, Gwen Lancashire and Ilona Kater for technical assistance in the field, James Weir and Ronald Balfour for



engineering and acquisitions support, and Carla Subke for assistance with the root severance experiment at Stirling. We thank  
585 Björn Lindahl (SLU Uppsala) for advice throughout the project.

### Financial support

Funding allocated by NERC NE/P002722/1 and NE/P002722/2; NEIF.

### Review statement

The review statement will be added by Copernicus Publications listing the handling editor as well as all contributing referees  
590 according to their status anonymous or identified.

### References

- Ascough, P., Bompard, N., Garnett, M. H., Gulliver, P., Murray, C., Newton, J. A., and Taylor, C.: 14c Measurement of  
Samples for Environmental Science Applications at the National Environmental Isotope Facility (Neif) Radiocarbon  
Laboratory, Suerc, Uk, Radiocarbon, 66, 1020-1031, 10.1017/rdc.2024.9, 2024.
- 595 Bardgett, R. D. and Cook, R.: Functional aspects of soil animal diversity in agricultural grasslands, Applied Soil Ecology, 10,  
263-276, [https://doi.org/10.1016/S0929-1393\(98\)00125-5](https://doi.org/10.1016/S0929-1393(98)00125-5), 1998.
- Becker, J. N. and Holz, M.: Hot or not? connecting rhizosphere hotspots to total soil respiration, Plant and Soil, 464, 489-499,  
2021.
- 600 Bernard, L., Basile-Doelsch, I., Derrien, D., Fanin, N., Fontaine, S., Guenet, B., Karimi, B., Marsden, C., and Maron, P. A.:  
Advancing the mechanistic understanding of the priming effect on soil organic matter mineralisation, Functional Ecology, 36,  
1355-1377, 10.1111/1365-2435.14038, 2022.
- Boutton, T. W., Wong, W. W., Hachey, D. L., Lee, L. S., Cabrera, M. P., and Klein, P. D.: Comparison of quartz and Pyrex  
tubes for combustion of organic samples for stable carbon isotope analysis, Analytical Chemistry, 55, 1832-1833,  
10.1021/ac00261a049, 1983.
- 605 Braghiere, R. K., Fisher, J. B., Miner, K. R., Miller, C. E., Worden, J. R., Schimel, D. S., and Frankenberg, C.: Tipping point  
in North American Arctic-Boreal carbon sink persists in new generation Earth system models despite reduced uncertainty,  
Environmental Research Letters, 18, 025008, 10.1088/1748-9326/acb226, 2023.
- Clemmensen, K. E., Durling, M. B., Michelsen, A., Hallin, S., Finlay, R. D., and Lindahl, B. D.: A tipping point in carbon  
storage when forest expands into tundra is related to mycorrhizal recycling of nitrogen, Ecol Lett, 24, 1193-1204,  
610 <https://doi.org/10.1111/ele.13735>, 2021.
- Clemmensen, K. E., Finlay, R. D., Dahlberg, A., Stenlid, J., Wardle, D. A., and Lindahl, B. D.: Carbon sequestration is related  
to mycorrhizal fungal community shifts during long-term succession in boreal forests, New Phytol, 205, 1525-1536,  
<https://doi.org/10.1111/nph.13208>, 2015.
- Crézé, C., Saatchi, S., Kwon, N., Yang, Y., and Li, S.: High-resolution global map (100 m) of soil organic carbon reveals  
critical ecosystems for carbon storage, Earth Syst. Sci. Data Discuss., 2025, 1-46, 10.5194/essd-2025-294, 2025.
- 615 Defrenne, C. E., Moore, J. A. M., Tucker, C. L., Lamit, L. J., Kane, E. S., Kolka, R. K., Chimner, R. A., Keller, J. K., and  
Lilleskov, E. A.: Peat loss collocates with a threshold in plant–mycorrhizal associations in drained peatlands encroached by  
trees, New Phytologist, 240, 412-425, <https://doi.org/10.1111/nph.18954>, 2023.
- Denis, E. H., Ilhardt, P. D., Tucker, A. E., Huggett, N. L., Rosnow, J. J., and Moran, J. J.: Spatially tracking carbon through  
the root–rhizosphere–soil system using laser ablation-IRMS, Journal of Plant Nutrition and Soil Science, 182, 401-410,  
620 <https://doi.org/10.1002/jpln.201800301>, 2019.



- Dial, R. J., Maher, C. T., Hewitt, R. E., Wockenfuss, A. M., Wong, R. E., Crawford, D. J., Zietlow, M. G., and Sullivan, P. F.: Arctic sea ice retreat fuels boreal forest advance, *Science*, 383, 877-884, <https://www.science.org/doi/10.1126/science.adh2339>, 2024.
- 625 Evans, C. D., Peacock, M., Baird, A. J., Artz, R. R. E., Burden, A., Callaghan, N., Chapman, P. J., Cooper, H. M., Coyle, M., Craig, E., Cumming, A., Dixon, S., Gauci, V., Grayson, R. P., Helfter, C., Heppell, C. M., Holden, J., Jones, D. L., Kaduk, J., Levy, P., Matthews, R., McNamara, N. P., Misselbrook, T., Oakley, S., Page, S. E., Rayment, M., Ridley, L. M., Stanley, K. M., Williamson, J. L., Worrall, F., and Morrison, R.: Overriding water table control on managed peatland greenhouse gas emissions, *Nature*, 593, 548-552, 10.1038/s41586-021-03523-1, 2021.
- 630 Fanin, N., Clemmensen, K. E., Lindahl, B. D., Farrell, M., Nilsson, M.-C., Gundale, M. J., Kardol, P., and Wardle, D. A.: Ericoid shrubs shape fungal communities and suppress organic matter decomposition in boreal forests, *New Phytologist*, 236, 684-697, <https://doi.org/10.1111/nph.18353>, 2022.
- Fernandez, C. W. and Kennedy, P. G.: Revisiting the 'Gadgil effect': do interguild fungal interactions control carbon cycling in forest soils?, *New Phytol*, 209, 1382-1394, <https://doi.org/10.1111/nph.13648>, 2016.
- 635 Friggens, N. L., Hester, A. J., Mitchell, R. J., Parker, T. C., Subke, J. A., and Wookey, P. A.: Tree planting in organic soils does not result in net carbon sequestration on decadal timescales, *Glob Chang Biol*, 26, 5178-5188, <https://doi.org/10.1111/gcb.15229>, 2020.
- Friggens, N. L., Hugelius, G., Kokelj, S. V., Murton, J. B., Phoenix, G. K., and Hartley, I. P.: Positive rhizosphere priming accelerates carbon release from permafrost soils, *Nature Communications*, 16, 3576, 10.1038/s41467-025-58845-9, 2025.
- 640 Garnett, M. H., Newton, J.-A., and Parker, T. C.: A Highly Portable and Inexpensive Field Sampling Kit for Radiocarbon Analysis of Carbon Dioxide, *Radiocarbon*, 63, 1355-1368, <https://doi.org/10.1017/RDC.2021.49>, 2021.
- Gaudinski, J. B., Trumbore, S.E., Davidson, E.A., Zheng, S.: Soil carbon cycling in a temperate forest: radiocarbon-based estimates of residence times, sequestration rates and partitioning of fluxes, *Biogeochemistry*, 51, 33-69, 2000.
- Gavazov, K., Albrecht, R., Buttler, A., Dorrepaal, E., Garnett, M. H., Gogo, S., Hagedorn, F., Mills, R. T. E., Robroek, B. J. M., and Bragazza, L.: Vascular plant-mediated controls on atmospheric carbon assimilation and peat carbon decomposition under climate change, *Glob Chang Biol*, 24, 3911-3921, 10.1111/gcb.14140, 2018.
- 645 Genney, D. R., Anderson, I. C., and Alexander, I. J.: Fine-scale distribution of pine ectomycorrhizas and their extramatrical mycelium, *New Phytologist*, 170, 381-390, <https://doi.org/10.1111/j.1469-8137.2006.01669.x>, 2006.
- Grelet, G. A., Johnson, D., Paterson, E., Anderson, I. C., and Alexander, I. J.: Reciprocal carbon and nitrogen transfer between an ericaceous dwarf shrub and fungi isolated from Piceirhiza bicolorata ectomycorrhizas, *New Phytol*, 182, 359-366, 10.1111/j.1469-8137.2009.02813.x, 2009.
- Hartley, I. P., Garnett, M. H., Sommerkorn, M., Hopkins, D. W., Fletcher, B. J., Sloan, V. L., Phoenix, G. K., and Wookey, P. A.: A potential loss of carbon associated with greater plant growth in the European Arctic, *Nature Climate Change*, 2, 875-879, 10.1038/nclimate1575, 2012.
- 655 ERA5 monthly averaged data on single levels from 1940 to present., last access: 25-03-2025.
- Hicks, L. C., Leizeaga, A., Rousk, K., Michelsen, A., and Rousk, J.: Simulated rhizosphere deposits induce microbial N-mining that may accelerate shrubification in the subarctic, *Ecology*, 101, e03094, 10.1002/ecy.3094, 2020.
- Huo, C., Luo, Y., and Cheng, W.: Rhizosphere priming effect: A meta-analysis, *Soil Biology and Biochemistry*, 111, 78-84, 10.1016/j.soilbio.2017.04.003, 2017.
- 660 Hutchinson, J. N.: The Record of Peat Wastage in the East Anglian Fenlands at Holme Post, 1848-1978 A.D, *Journal of Ecology*, 68, 229-249, 10.2307/2259253, 1980.
- Keuper, F., Wild, B., Kummu, M., Beer, C., Blume-Werry, G., Fontaine, S., Gavazov, K., Gentsch, N., Guggenberger, G., Hugelius, G., Jalava, M., Koven, C., Krab, E. J., Kuhry, P., Monteux, S., Richter, A., Shahzad, T., Weedon, J. T., and Dorrepaal, E.: Carbon loss from northern circumpolar permafrost soils amplified by rhizosphere priming, *Nature Geoscience*, 13, 560-565, 10.1038/s41561-020-0607-0, 2020.
- 665 Kuhry, P., Grosse, G., Harden, J. W., Hugelius, G., Koven, C. D., Ping, C. L., Schirmer, L., and Tarnocai, C.: Characterisation of the Permafrost Carbon Pool, *Permafrost and Periglacial Processes*, 24, 146-155, 10.1002/ppp.1782, 2013.
- Kuzyakov, Y.: Priming effects: Interactions between living and dead organic matter, *Soil Biology and Biochemistry*, 42, 1363-1371, <https://doi.org/10.1016/j.soilbio.2010.04.003>, 2010.
- 670 Kuzyakov, Y. and Blagodatskaya, E.: Microbial hotspots and hot moments in soil: Concept & review, *Soil Biology and Biochemistry*, 83, 184-199, <https://doi.org/10.1016/j.soilbio.2015.01.025>, 2015.



- Lindahl, B. D. and Tunlid, A.: Ectomycorrhizal fungi - potential organic matter decomposers, yet not saprotrophs, *New Phytol*, 205, 1443-1447, 10.1111/nph.13201, 2015.
- 675 Martino, E., Morin, E., Grelet, G. A., Kuo, A., Kohler, A., Daghino, S., Barry, K. W., Cichocki, N., Clum, A., Dockter, R. B., Hainaut, M., Kuo, R. C., LaButti, K., Lindahl, B. D., Lindquist, E. A., Lipzen, A., Khouja, H. R., Magnuson, J., Murat, C., Ohm, R. A., Singer, S. W., Spatafora, J. W., Wang, M., Veneault-Fourrey, C., Henrissat, B., Grigoriev, I. V., Martin, F. M., and Perotto, S.: Comparative genomics and transcriptomics depict ericoid mycorrhizal fungi as versatile saprotrophs and plant mutualists, *New Phytol*, 217, 1213-1229, <https://doi.org/10.1111/nph.14974>, 2018.
- 680 Michaud, T., Hobbie, E., and Kennedy, P.: Carbon cycling through plant and fungal herbarium specimens tracks the Sues effect over more than a century of environmental change, *Fungal Ecology*, 71, 101372, <https://doi.org/10.1016/j.funeco.2024.101372>, 2024.
- Mielke, L. A., Klein, J., Ekblad, A., Finlay, R. D., Lindahl, B. D., and Clemmensen, K. E.: Fungal guild interactions slow decomposition of boreal forest pine litter and humus, *New Phytologist*, 247, 2367-2380, <https://doi.org/10.1111/nph.70316>, 2025.
- 685 Miyauchi, S., Kiss, E., Kuo, A., Drula, E., Kohler, A., Sánchez-García, M., Morin, E., Andreopoulos, B., Barry, K. W., Bonito, G., Buée, M., Carver, A., Chen, C., Cichocki, N., Clum, A., Culley, D., Crous, P. W., Fauchery, L., Girlanda, M., Hayes, R. D., Kéri, Z., LaButti, K., Lipzen, A., Lombard, V., Magnuson, J., Maillard, F., Murat, C., Nolan, M., Ohm, R. A., Pangilinan, J., Pereira, M. d. F., Perotto, S., Peter, M., Pfister, S., Riley, R., Sitrit, Y., Stielow, J. B., Szöllösi, G., Žifčáková, L., Štursová, M., Spatafora, J. W., Tedersoo, L., Vaario, L.-M., Yamada, A., Yan, M., Wang, P., Xu, J., Bruns, T., Baldrian, P., Vilgalys, R., Dunand, C., Henrissat, B., Grigoriev, I. V., Hibbett, D., Nagy, L. G., and Martin, F. M.: Large-scale genome sequencing of mycorrhizal fungi provides insights into the early evolution of symbiotic traits, *Nature Communications*, 11, 5125, 10.1038/s41467-020-18795-w, 2020.
- 690 Mueller, P. and Megonigal, J. P.: Redox control on rhizosphere priming in wetlands, *Nature Geoscience*, 17, 1209-1217, 10.1038/s41561-024-01584-1, 2024.
- 695 Packard, E. E., Pérez-Izquierdo, L., Clemmensen, K. E., Dahlberg, A., Spohn, M., Stendahl, J., and Lindahl, B. D.: Ectomycorrhizal decomposers and their niche(s) in boreal forests, *Functional Ecology*, n/a, <https://doi.org/10.1111/1365-2435.70085>, 2025.
- Parker, T. C., Subke, J.-A., and Wookey, P. A.: Rapid carbon turnover beneath shrub and tree vegetation is associated with low soil carbon stocks at a subarctic treeline, *Global Change Biology*, 21, 2070-2081, <https://doi.org/10.1111/gcb.12793>, 2015.
- 700 Parker, T. C., Evans, C., Evans, M. G., Glendell, M., Grayson, R., Holden, J., Li, C., Li, P., and Artz, R. R. E.: Ideas and Perspectives: Potentially Large but Highly Uncertain Greenhouse Gas Emissions Resulting from Peat Erosion, *EGUsphere*, 2025, 1-13, 10.5194/egusphere-2025-287, 2025.
- Parker, T. C., Clemmensen, K. E., Friggens, N. L., Hartley, I. P., Johnson, D., Lindahl, B. D., Olofsson, J., Siewert, M. B., Street, L. E., Subke, J. A., and Wookey, P. A.: Rhizosphere allocation by canopy-forming species dominates soil CO<sub>2</sub> efflux in a subarctic landscape, *New Phytol*, 227, 1818-1830, <https://doi.org/10.1111/nph.16573>, 2020.
- 705 Parker, T. C., Chomel, M., Clemmensen, K. E., Friggens, N. L., Hartley, I. P., Johnson, D., Kater, I., Krab, E. J., Lindahl, B. D., Street, L. E., Subke, J. A., and Wookey, P. A.: Resistance of subarctic soil fungal and invertebrate communities to disruption of below-ground carbon supply, *Journal of Ecology*, 110, 2883-2897, <https://doi.org/10.1111/1365-2745.13994>, 2022.
- 710 Paterson, E., Midwood, A. J., and Millard, P.: Through the eye of the needle: a review of isotope approaches to quantify microbial processes mediating soil carbon balance, *New Phytologist*, 184, 19-33, <https://doi.org/10.1111/j.1469-8137.2009.03001.x>, 2009.
- Rantanen, M., Karpechko, A. Y., Lipponen, A., Nordling, K., Hyvärinen, O., Ruosteenoja, K., Vihma, T., and Laaksonen, A.: The Arctic has warmed nearly four times faster than the globe since 1979, *Communications Earth & Environment*, 3, 168, 10.1038/s43247-022-00498-3, 2022.
- 715 Read, D. J. and Perez-Moreno, J.: Mycorrhizas and nutrient cycling in ecosystems – a journey towards relevance?, *New Phytologist*, 157, 475-492, 10.1046/j.1469-8137.2003.00704.x, 2003.
- Rees, W. G., Hofgaard, A., Boudreau, S., Cairns, D. M., Harper, K., Mamet, S., Mathisen, I., Swirad, Z., and Tutubalina, O.: Is subarctic forest advance able to keep pace with climate change?, *Glob Chang Biol*, 26, 3965-3977, <https://doi.org/10.1111/gcb.15113>, 2020.
- 720



- Rosling, A., Landeweert, R., Lindahl, B. D., Larsson, K. H., Kuyper, T. W., Taylor, A. F. S., and Finlay, R. D.: Vertical distribution of ectomycorrhizal fungal taxa in a podzol soil profile, *New Phytol*, 159, 775-783, 10.1046/j.1469-8137.2003.00829.x, 2003.
- 725 Siles, J. A., Díaz-López, M., Vera, A., Eisenhauer, N., Guerra, C. A., Smith, L. C., Buscot, F., Reitz, T., Breitzkreuz, C., van den Hoogen, J., Crowther, T. W., Orgiazzi, A., Kuzyakov, Y., Delgado-Baquerizo, M., and Bastida, F.: Priming effects in soils across Europe, *Global Change Biology*, 28, 2146-2157, <https://doi.org/10.1111/gcb.16062>, 2022.
- Sloan, T. J., Payne, R. J., Anderson, A. R., Gilbert, P., Mauquoy, D., Newton, A., and Andersen, R.: Ground surface subsidence in an afforested peatland fifty years after drainage and planting, *Mires and Peat*, 2019.
- 730 Sloan, V. L., Fletcher, B. J., Press, M. C., Williams, M., and Phoenix, G. K.: Leaf and fine root carbon stocks and turnover are coupled across Arctic ecosystems, *Glob Chang Biol*, 19, 3668-3676, 10.1111/gcb.12322, 2013.
- Smith, S. E. and Read, D. J.: *Mycorrhizal symbiosis*, Academic press, 2008.
- Solly, E.F., Brunner, I., Helmisaari, H. S. *et al.* Unravelling the age of fine roots of temperate and boreal forests, *Nat Comms*, 9, 3006, <https://doi.org/10.1038/s41467-018-05460-6>, 2018.
- 735 Sterkenburg, E., Clemmensen, K. E., Ekblad, A., Finlay, R. D., and Lindahl, B. D.: Contrasting effects of ectomycorrhizal fungi on early and late stage decomposition in a boreal forest, *ISME J*, 12, 2187-2197, 10.1038/s41396-018-0181-2, 2018.
- Street, L. E., Garnett, M. H., Subke, J. A., Baxter, R., Dean, J. F., and Wookey, P. A.: Plant carbon allocation drives turnover of old soil organic matter in permafrost tundra soils, *Global Change Biology*, 26, 4559-4571, 10.1111/gcb.15134, 2020.
- Stuiver, M. and Polach, H. A.: Discussion Reporting of 14C Data, *Radiocarbon*, 19, 355-363, 10.1017/S0033822200003672, 1977.
- 740 Subke, J.-A., Reichstein, M., and Tenhunen, J. D.: Explaining temporal variation in soil CO<sub>2</sub> efflux in a mature spruce forest in Southern Germany, *Soil Biology and Biochemistry*, 35, 1467-1483, 2003.
- UNEP, U. N. E. P.: One health joint plan of action (2022–2026): working together for the health of humans, animals, plants and the environment, World Health Organization, 2022.
- 745 Wild, B., Monteux, S., Wendler, B., Hugelius, G., and Keuper, F.: Circum-Arctic peat soils resist priming by plant-derived compounds, *Soil Biology and Biochemistry*, 180, 109012, <https://doi.org/10.1016/j.soilbio.2023.109012>, 2023.
- Wild, B., Gentsch, N., Capek, P., Diakova, K., Alves, R. J., Barta, J., Gittel, A., Hugelius, G., Knoltsch, A., Kuhry, P., Lashchinskiy, N., Mikutta, R., Palmtag, J., Schleper, C., Schneckner, J., Shibistova, O., Takriti, M., Torsvik, V. L., Urich, T., Watzka, M., Santruckova, H., Guggenberger, G., and Richter, A.: Plant-derived compounds stimulate the decomposition of organic matter in arctic permafrost soils, *Sci Rep*, 6, 25607, 10.1038/srep25607, 2016.
- 750 Wilmking, M., Harden, J., and Tape, K.: Effect of tree line advance on carbon storage in NW Alaska, *Journal of Geophysical Research: Biogeosciences*, 111, n/a-n/a, 10.1029/2005jg000074, 2006.
- Zuev, A. G., Potapov, M. B., Tiunov, A. V., and Saraeva, A. K.: Root trenching and stable isotope analysis uncover trophic links of euedaphic collembola species to mycorrhizal mycelium in pine forests, *European Journal of Soil Biology*, 118, 103519, <https://doi.org/10.1016/j.ejsobi.2023.103519>, 2023.

755